Letter

Bernoulli trial under restarts: A comparative study of resetting transitions

R. K. Singh [1,*] T. Sandev [2,3,4,†] and Sadhana Singh [5,‡]

[1]*Department of Physics, Bar-Ilan University, Ramat-Gan 5290002, Israel*

[2]*Research Center for Computer Science and Information Technologies, Macedonian Academy of Sciences and Arts, Bul. Krste Misirkov 2, 1000 Skopje, Macedonia*

[3]*Institute of Physics & Astronomy, University of Potsdam, D-14776 Potsdam-Golm, Germany*

[4]*Institute of Physics, Faculty of Natural Sciences and Mathematics, Ss. Cyril and Methodius University, Arhimedova 3, 1000 Skopje, Macedonia*

[5]*The Avram and Stella Goldstein-Goren Department of Biotechnology Engineering, Ben-Gurion University of the Negev, Be'er Sheva 84105, Israel*

(Received 2 May 2023; accepted 23 October 2023; published 21 November 2023)

A Bernoulli trial describing the escape behavior of a lamb to a safe haven in pursuit by a lion is studied under restarts. The process ends in two ways: either the lamb makes it to the safe haven (success) or is captured by the lion (failure). We study the first passage properties of this Bernoulli trial and find that only mean first passage time exists. Considering Poisson and sharp resetting, we find that the success probability is a monotonically decreasing function of the restart rate. The mean time, however, exhibits a nonmonotonic dependence on the restart rate taking a minimal value at an optimal restart rate. Furthermore, for sharp restart, the mean time possesses a local and a global minima. As a result, the optimal restart rate exhibits a continuous transition for Poisson resetting while it exhibits a discontinuous transition for sharp resetting as a function of the relative separation of the lion and the lamb. We also find that the distribution of first passage times under sharp resetting exhibits a periodic behavior.

DOI: 10.1103/PhysRevE.108.L052106

Introduction. Bernoulli trials are ubiquitous in nature, with examples ranging from the gambler ruin problem [1], multiple targets in confined geometries [2–4], mortal random walkers [5–9], chemical selectivity [10], multiple folding options for a biopolymer [11,12], to mention a few. A stochastic process is termed as a Bernoulli trial if it can end in two ways and for such processes it is not unusual to designate a desired outcome of the trial as success and the remaining outcome(s) as failure(s).

A well-studied example of a Bernoulli trial comes from the realm of capture processes [13–19] wherein a hungry lion pursues a lamb and the lamb has the lifesaving opportunity to make it to a safe haven [20]. Furthermore, capture processes have applications ranging from reaction systems [21–23] to population dynamics [24] to kinetochore capture by spindle molecules [25], making it imperative to study the properties of such Bernoulli trials like in Ref. [20] under resetting. This becomes particularly important in light of the fact that the success probability of a Bernoulli trial can be optimized via restarts [26]. In the present work, we study the Bernoulli trial described in Ref. [20] in presence of restarts. Describing the lion and the lamb as vicious walkers, which destroy each other the moment their paths cross [27–35], we study the system of two vicious walkers under restarts. This is further corroborated from the fact that the viciousness property $A + A \to \emptyset$ [36–40] has been previously applied to study the classic lion-lamb capture problem [16,41,42].

In the present work, we employ two restart protocols: one in which the rate of restart is fixed, aka, Poissonian resetting [43–54]; and the other in which the time between two restarts is fixed, aka sharp restarts [55–62]. The reason for covering these two restart protocols is that they lie at the two extremes of the class of renewal restart protocols: Poissonian resetting being memoryless and sharp restart retaining its entire memory. Notwithstanding the extensive literature addressing the effects of both Poissonian and sharp restarts, studies addressing stochastic processes ending in more than one way have been rather limited [26,57,63] and specific examples addressing the effect of sharp restarts on Bernoulli trials is still missing, to the best of our knowledge.

Two vicious random walkers with an absorbing wall. Consider a pair of vicious Brownian particles on the positive half-line with $0 < x_1 < x_2 < \infty$ [20]. The process ends when either the first walker reaches the haven at $x_1 = 0$ (success) or when the trajectories of the two particles cross each other, that is $x_1 = x_2$, at which point the two vicious walkers kill each other (failure). The Fokker-Planck equation (FPE) describing the probability density function (PDF) of the process is

$$\partial_t p = D_1 \partial_1^2 p + D_2 \partial_2^2 p, \tag{1}$$

*rksinghmp@gmail.com
†trifce.sandev@manu.edu.mk
‡sdhnsingh080@gmail.com

where $\partial_t \equiv \frac{\partial}{\partial t}$, $\partial_i^2 \equiv \frac{\partial^2}{\partial x_i^2}$, $i = 1, 2$, and $p \equiv p(x_1, x_2, t)$. The initial condition for the FPE in (1) is $p(x_1, x_2, 0) = \delta(x_1 - c_1)\delta(x_2 - c_2)$ with $c_1 < c_2$ along with the boundary conditions $p(x_1 = 0, x_2 = x > 0, t) = 0$ (the lamb reaching the haven) and $p(x_1 = x, x_2 = x, t) = 0$ (lion kills the lamb). Without any loss of generality we assume that the two Brownian particles have identical diffusion coefficients, that is, $D_1 = D_2 = D$. The FPE in Eq. (1) can be solved using the method of images and its solution is the antisymmetric linear combination (see Fig. 5 in Ref. [27]):

$$\begin{aligned} p(x_1, x_2, t) = {} & f(x_1, x_2, t) - f(x_2, x_1, t) - f(-x_1, x_2, t) \\ & + f(x_2, -x_1, t) - f(-x_2, -x_1, t) \\ & + f(-x_1, -x_2, t) - f(x_1, -x_2, t) \\ & + f(-x_2, x_1, t), \end{aligned} \tag{2}$$

where $f(x_1, x_2, t) = \frac{1}{4\pi Dt} \exp\left[-\frac{(x_1-c_1)^2+(x_2-c_2)^2}{4Dt}\right]$ is the PDF of a pair of noninteracting Brownian particles in one dimension. It is straightforward to see that $p(x_1, x_2, t)$ satisfies the initial and boundary conditions complementing Eq. (1).

First passage time distribution. The PDF in (2) allows us to estimate the survival probability: $q(t) = \int_0^\infty dx_1 \int_{x_1}^\infty dx_2 p(x_1, x_2, t)$ and from there the first passage time distribution (FPTD) reads $F(t) = -\frac{d}{dt}q(t) = -D[\int_0^\infty dx_2 \frac{\partial p}{\partial x_1}|_0^{x_2} + \int_0^\infty dx_1 \frac{\partial p}{\partial x_2}|_{x_1}^\infty]$ leading to

$$\begin{aligned} F(t) = {} & \frac{1}{\sqrt{4\pi Dt^3}}\left[c_1 \mathrm{erf}\left(\frac{c_2}{\sqrt{4Dt}}\right)\exp\left(-\frac{c_1^2}{4Dt}\right)\right. \\ & \left. - c_2 \mathrm{erf}\left(\frac{c_1}{\sqrt{4Dt}}\right)\exp\left(-\frac{c_2^2}{4Dt}\right)\right] + \frac{1}{\sqrt{8\pi Dt^3}} \\ & \times \left\{(c_2 - c_1)\mathrm{erf}\left(\frac{c_1 + c_2}{\sqrt{8Dt}}\right)\exp\left[-\frac{(c_1 - c_2)^2}{8Dt}\right]\right. \\ & \left. - (c_1 + c_2)\mathrm{erf}\left(\frac{c_2 - c_1}{\sqrt{8Dt}}\right)\exp\left[-\frac{(c_1 + c_2)^2}{8Dt}\right]\right\}. \end{aligned} \tag{3}$$

The integral leading to Eq. (3) above has been evaluated using MAXIMA. Using the small argument approximation for the exponential and error function we have $F(t) \overset{t\to\infty}{\sim} 1/\pi t^3$. As a result, $q(t) \overset{t\to\infty}{\sim} 1/t^2$, previously derived using a wedge domain in Ref. [20]. This implies that the unconditional mean first passage time (MFPT) is finite, and in addition, it is the only finite moment possessed by the FPTD in Eq. (3). From this we can write the expressions for the conditional FPTDs, the process terminating either in a success or failure. Define $F_1(t)$ as the distribution of first passage times that the process ends when the first particle reaches the origin irrespective of the location of the second particle, that is, a successful completion of the Bernoulli process. Similarly, let $F_2(t)$ denote the conditional FPTD for the process to end by the two vicious walkers killing each other, that is, a failure. Then, $F(t) = F_1(t) + F_2(t)$ and from Eq. (3) we obtain:

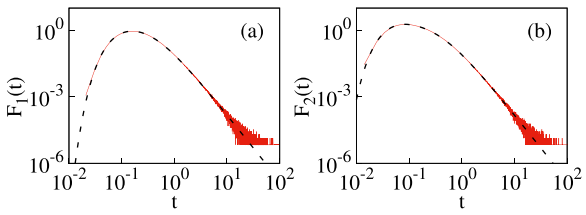

FIG. 1. Conditional FPTDs $F_1(t)$ and $F_2(t)$ for the pair of vicious Brownian particles. The red line is the numerical estimate and the black dashed lines are the expressions from Eq. (4). Parameter values are $c_1 = 1$, $c_2 = 2$, $D = 1$. For these values: $\mathcal{E}_1 = \int_0^\infty dt\, F_1(t) \approx 0.41$ (see Ref. [64] for details).

$$\begin{aligned} F_1(t) = {} & \frac{1}{\sqrt{4\pi Dt^3}}\left[c_1 \mathrm{erf}\left(\frac{c_2}{\sqrt{4Dt}}\right)\exp\left(-\frac{c_1^2}{4Dt}\right)\right. \\ & \left. - c_2 \mathrm{erf}\left(\frac{c_1}{\sqrt{4Dt}}\right)\exp\left(-\frac{c_2^2}{4Dt}\right)\right], \end{aligned} \tag{4a}$$

$$\begin{aligned} F_2(t) = {} & \frac{1}{\sqrt{8\pi Dt^3}}\left\{(c_2 - c_1)\mathrm{erf}\left(\frac{c_1 + c_2}{\sqrt{8Dt}}\right)\right. \\ & \times \exp\left[-\frac{(c_1 - c_2)^2}{8Dt}\right] \\ & \left. - (c_1 + c_2)\mathrm{erf}\left(\frac{c_2 - c_1}{\sqrt{8Dt}}\right)\exp\left[-\frac{(c_1 + c_2)^2}{8Dt}\right]\right\}. \end{aligned} \tag{4b}$$

We find that the analytical result for the FPTD in Eq. (4) agrees well with numerical calculations (see Fig. 1 and Ref. [64] for details).

Restarting the Bernoulli process. For reasons discussed in Ref. [65], we reset the two vicious walkers at the exact same moment. Furthermore, the time between two successive restarts is chosen for the purpose of simplicity to be either an exponentially distributed random variable (Poissonian resetting) or a fixed quantity (sharp resetting). In order to compare Poissonian and sharp restart for the Bernoulli trial under consideration, let us define $1/\tau$ as the rate of sharp restart, where τ is the time of sharp restart. This definition puts the two restart protocols on same footing and we define

$$\rho = \begin{cases} r, & \text{for Poisson restart,} \\ 1/\tau, & \text{for sharp restart.} \end{cases} \tag{5}$$

Now, if T is the time of unconditional completion of the Bernoulli trial under consideration and R is the time of restart of the process, then the success probability is: $p = \frac{\langle I(T<R) y_T \rangle}{\langle I(T<R) \rangle}$ [26], where y_T is an auxiliary random variable taking value one with probability $F_1(t)/F(t)$. And, if $\langle T^s \rangle$ is the conditional MFPT for a successful trial, then $\langle T^s \rangle = \frac{\langle I(T>R)R \rangle}{\langle I(T<R) \rangle} + \frac{\langle I(T<R) y_T T \rangle}{\langle I(T<R) y_T \rangle}$ [26]. Let us now discuss Poisson and sharp restart protocols one by one.

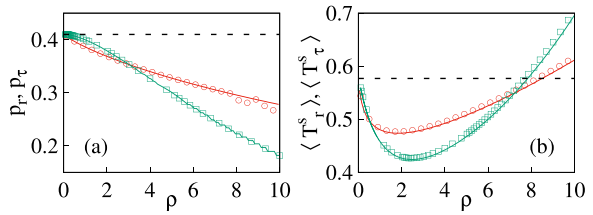

FIG. 2. Effect of restarts: (a) Numerically estimated probability of success under Poisson restart $p_r(\circ)$ and sharp restart $p_\tau(\square)$ vs the corresponding analytical results [Eqs. (6a) and (7)]. (b) Numerically estimated conditional MFPT under Poisson restart $\langle T_r^s \rangle(\circ)$ and sharp restart $\langle T_\tau^s \rangle(\square)$ vs the corresponding analytical results in solid lines [Eqs. (6b) and (8)]. Parameter values are $c_1 = 1$, $c_2 = 2$, $D = 1$ and black dashed lines represent the limit of no restarts.

For Poissonian resetting at a rate r, the PDF of restart times is $P^r(R) = re^{-rR}$. As a result, the success probability and the conditional MFPT, respectively, read [26]:

$$p_r = \frac{\tilde{F}_1(r)}{\tilde{F}(r)}, \tag{6a}$$

$$\langle T_r^s \rangle = \langle T_r \rangle - \frac{d}{dr} \ln p_r, \tag{6b}$$

where $\langle T_r \rangle = \frac{1-\tilde{F}(r)}{r\tilde{F}(r)}$ [66] denotes the mean time of completion of the Bernoulli trial, either with a success or as a failure; and $\tilde{F}(r) = \int_0^\infty dt\, e^{-rt} F(t)$ is the Laplace transform of $F(t)$. We see from Fig. 2(a) that p_r is a monotonically decreasing function of the restart rate r, while the conditional MFPT for a successful completion $\langle T_r^s \rangle$ exhibits a minima, as seen from Fig. 2(b). This implies that while resetting makes it slightly less probable for the lamb to make it to the safe haven, the time to reach the safe haven can be minimal, for example, for $r \approx 2$. For higher values of restart rate such as $r \approx 10$, the lamb is walking a slippery slope where it takes a longer time to reach the haven and the chances of it doing so are also severely diminished, thanks to the fact that it keeps returning home. It should be noted at this point that the Laplace transforms in Eq. (6) have been evaluated via numerical integration [67]. Let us now move on to studying the Bernoulli trial under sharp resetting.

For sharp resetting the PDF of restart times is $P^\tau(R) = \delta(R - \tau)$, where τ is the time of sharp restart. Then $\langle I(T < R) y_T \rangle = \int_0^\infty dR P^\tau(R) \int_0^\infty dt F(t) I(T < R) y_T = \int_0^\infty dt F_1(t) \int_t^\infty dR \delta(R - \tau) = \int_0^\tau dt F_1(t)$ where we have reversed the order of integration in the second equality and the δ-function term contributes only when $t \leqslant \tau$. In a similar manner we have $\langle I(T < R) \rangle = \int_0^\tau dt\, F(t)$, from which follows the success probability under sharp resetting

$$p_\tau = \frac{\int_0^\tau dt\, F_1(t)}{\int_0^\tau dt\, F(t)}. \tag{7}$$

Evaluating the remaining integrals we get $\langle I(T > R) R \rangle = \tau \int_\tau^\infty dt F(t)$ and $\langle I(T < R) y_T T \rangle = \int_0^\tau dt t F_1(t)$ leading to the conditional MFPT under sharp restarts:

$$\langle T_\tau^s \rangle = \frac{\tau \int_\tau^\infty dt\, F(t)}{\int_0^\tau dt\, F(t)} + \frac{\int_0^\tau dt\, t F_1(t)}{\int_0^\tau dt\, F_1(t)}. \tag{8}$$

We see in Fig. 2 that the success probability under sharp restarts p_τ asymptotically approaches its value in absence of any restarts in a monotonic way and remains less than $\lim_{\tau\to\infty} p_\tau$ [see Fig. 2(a)]. On the other hand, the mean time taken by the lamb to successfully reach the safe haven $\langle T_\tau^s \rangle$ exhibits a nonmonotonic dependence (in sharp contrast with p_τ) on the restart time τ. This implies that sharp resetting is advantageous for the lamb as it is able to quickly take resort to the safe haven as compared to the case when there are no restarts. Unlike its Poissonian counterpart, a sharp restart of the Bernoulli trial with high value of τ is advantageous for the lamb, as its probability to make it to the safe haven is close to $\mathcal{E}_1$, and this mode of completion takes a lesser amount of time on average. This prompts us to make an explicit comparison between the two restart protocols, and more so their relation to the dynamics of the Bernoulli trial without restarts. We proceed with this goal in the next section.

Comparing Poissonian restart with sharp restart. As we have seen above, for both Poisson and sharp restart protocols, we have $\lim_{r\to 0} p_r = \lim_{\tau\to\infty} p_\tau = \mathcal{E}_1$. This is also seen in Fig. 2(a) for ρ in the neighborhood of zero. However, the approach of p_r and p_τ to $\mathcal{E}_1$ is completely different in that the second derivative $d^2p/d\rho^2$ near $\rho \approx 0$ is positive or negative depending on whether we consider Poisson or sharp restart protocol [see Fig. 2(a)]. This can be understood as follows. For sharp restart ρ near zero means that the time interval between two successive restarts τ is very large, which means that the Bernoulli trial stops without being practically perturbed by any restart event [see the near-horizontal behavior of p for small ρ in Fig. 2(a)]. On the other hand, since $\langle T \rangle < \langle T^s \rangle$ [from Eqs. (3) and (4a)], we have for Poissonian restarts: $p_r \overset{r\to 0}{\sim} \mathcal{E}_1 + \mathcal{E}_1(\langle T \rangle - \langle T^s \rangle) r$, which leads to $dp_r/dr < 0$ for $r \to 0$. Note that we can take this analysis no further as the higher-order moments of the FPTD $F(t)$ do not exist. The difference in the signs of the second derivative of success probability eventually lead to $p_\tau < p_r$ for large ρ with $\lim_{\rho\to\infty} p = 0$ [see inset in Fig. 2(a)]. This follows simply from the fact that for large ρ both the vicious walkers are reset to their initial locations very rapidly, making it practically impossible for the lamb to make it to the safe haven.

It is further evident from Fig. 2(b) that the conditional MFPT under restarts, viz. both $\langle T_r^s \rangle$ and $\langle T_\tau^s \rangle$ exhibit a nonmonotonic dependence on the restart rate ρ. Let ρ_0 denote the optimal resetting rate (ORR) at which the mean time attains its minimal value. We study the properties of the ORR for both Poisson and sharp restarts in Fig. 3 as a function of the initial locations of the lamb c_1 and the lion c_2. When studying the dependence of the inverse ORR $1/\rho_0$ as a function of c_1, a natural length scale in the system is c_2, and the corresponding time scale is c_2^2/D. We thus measure the initial location of the lamb in units of c_2, and the inverse ORR in units of c_2^2/D. We employ a similar procedure when studying $1/\rho_0$ as a function of c_2 (see Fig. 3). Following this scaling we find that the data for the inverse ORR $1/\rho_0$ for different sets of motion parameters collapse on top of each other for both Poisson [Figs. 3(a) and 3(b)] and sharp restarts [Figs. 3(c) and 3(d)]. This implies that $1/\rho_0$ exhibits a dynamical phase transition as a function of the relative separation of the two vicious walkers. Furthermore, independent of the nature of

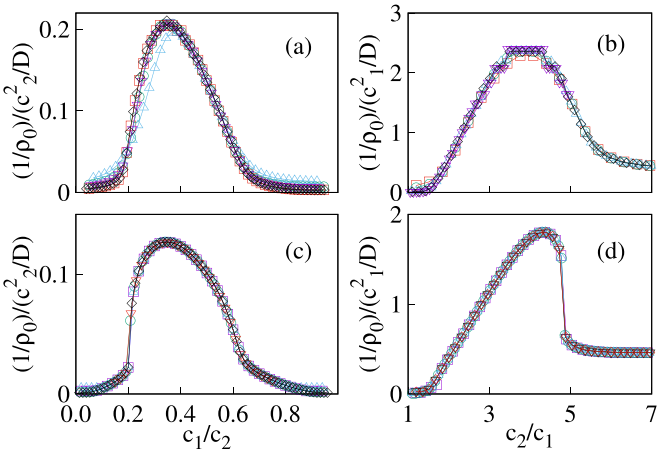

FIG. 3. For Poisson restarts (a) normalized ORR $(1/\rho_0)/(c_2^2/D)$ as a function of the normalized initial location of the first particle c_1/c_2 with $(c_2, D) = (2, 1)(\square)$, $(2, 2)(\circ)$, $(1.5, 2)(\triangle)$, $(1.8, 1.5)(\triangledown)$, $(2.5, 1.5)(\diamond)$; and (b) normalized ORR $(1/\rho_0)/(c_1^2/D)$ as a function of the normalized initial location of the second particle c_2/c_1 with $(c_1, D) = (0.5, 1.5)(\square)$, $(0.5, 1.0)(\circ)$, $(1.3, 2)(\triangle)$, $(2, 2.5)(\triangledown)$, $(1, 0.8)(\diamond)$. For sharp restarts (c) normalized ORR $(1/\rho_0)/(c_2^2/D)$ as a function of the normalized initial location of the first particle c_1/c_2 with $(c_2, D) = (2, 1)(\square)$, $(2.5, 1)(\circ)$, $(2, 2)(\triangle)$, $(2, 4)(\triangledown)$, $(3, 1)(\diamond)$; and (d) normalized ORR $(1/\rho_0)/(c_1^2/D)$ as a function of the normalized initial location of the second particle c_2/c_1 with $(c_1, D) = (0.6, 1)(\square)$, $(1, 1)(\circ)$, $(1, 2)(\triangle)$, $(0.5, 2)(\triangledown)$, $(0.5, 1.5)(\diamond)$. Data collapse for different sets of parameters implies that the ORR varies continuously for Poisson restarts while it exhibits a jump for sharp restarts.

the restart protocol, the optimal value of the mean restart time $1/\rho_0$ decreases when the lamb starts either very close to the safe haven at $x = 0$ or close to the initial location of the lion. This is because when the lamb starts close to the safe haven, that is $c_1/c_2 \ll 1$, then for restart to be useful the mean restart time should be less as the mean time to escape to the safe haven is already small. On the other hand, when the lamb starts close to the lion, that is, $c_1/c_2 \lesssim 1$, then if the process does not restart quickly, then it is more likely that the lion captures the lamb [see Figs. 3(a) and 3(c)]. This holds true even when we see this from the perspective of the lion, that is, mean time of optimal restart $1/\rho_0$ is small when $c_2/c_1 \gtrsim 1$. In the other extreme when the initial separation between the lamb and the lion is very large, that is, $c_2/c_1 \gg 1$, then once again $1/\rho_0$ is small [see Figs. 3(b) and 3(d)]. This is because in the limit $c_2/c_1 \gg 1$, chances of the lamb escaping to the safe haven are fairly high (without any restart) thus requiring rapid restart events for the protocol to be of any significance. In summary, Fig. 3 describes the resetting transition exhibited by $1/\rho_0$ as a function of relative separation c_1/c_2. The phase boundary separates the regions of the parameter space in which restart is useful from those in which it is not. The two domains of the parameter space are $c_1/c_2 \in (0, 1)$ and $c_2/c_1 \in (1, \infty)$. There is, however, one crucial difference between the phase boundaries of the two restart protocols. While the curve for Poisson restarts is continuous in both the intervals, that is, $0 < c_1/c_2 < 1$ and $c_2/c_1 > 1$, the corresponding curve

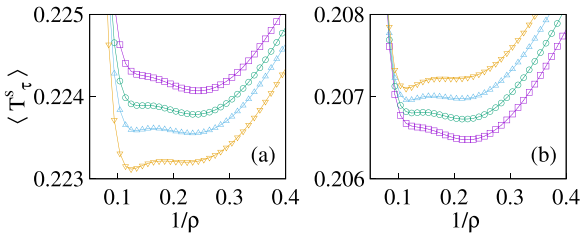

FIG. 4. Conditional MFPT under sharp restart $\langle T_\tau^s \rangle$ as a function of (a) $c_1 = 0.4167(\square), 0.4162(\circ), 0.4158(\triangle), 0.4152(\triangledown)$ for $c_2 = 2$; (b) $c_2 = 1.92(\square), 1.9225(\circ), 1.925(\triangle), 1.9275(\triangledown)$ for $c_1 = 0.4$. In both the cases $D = 1$.

under sharp resetting exhibits a jump discontinuity, in both the intervals. This marks a fundamental difference between the two restart protocols, that is, the ORR (or rather its inverse $1/\rho_0$) exhibits a continuous dynamical phase transition as a function of the relative initial separation of the walkers for Poisson restarts while for sharp restarts the resetting transition is discontinuous. The location of the jump discontinuity for sharp resetting is at $c_1/c_2 \approx 0.2$ in Fig. 3(c) or $c_2/c_1 \approx 5$ in Fig. 3(d), reflecting the fact that the location of jump depends only on the relative separation between the two vicious walkers.

In order to understand the discontinuous nature of the resetting transition for sharp restarts we study in detail the behavior of $\langle T_\tau^s \rangle$ as a function of initial locations of the lamb c_1 and the lion c_2. In Fig. 4 we see that $\langle T_\tau^s \rangle$ exhibits a bimodal behavior as a function of the initial locations c_1/c_2: with one local minima and one global minima. The two switch positions as we change c_i for a fixed c_j $(i \neq j)$. For example, in Fig. 4(a), when the initial location of the lamb c_1 is varied (for a fixed c_2), we see that a decreasing c_1 shifts the global minima from $1/\rho \approx 0.224$ to $1/\rho \approx 0.124$, a significant change leading to a jump in the value of $1/\rho_0$ observed in Fig. 3(c). A similar jump in the location of global minima $1/\rho_0$ is observed in Fig. 4(b), going from $1/\rho \approx 0.224$ to $1/\rho \approx 0.114$, when the initial location of the lion c_2 is increased (for a fixed c_1). It is important to notice from Fig. 4 that the location of the global minima $1/\rho_0$ goes to lower values with increasing relative separation, occurring either due to the lamb starting closer to the safe haven or the lion starting farther from the lamb. This switching of the location of global minima leads to a discontinuous resetting transition for sharp restarts.

Let us now discuss the effect of resetting on the FPTD $F(t)$. Under Poissonian resetting at a rate r, the FPTD is known to be: $\tilde{F}_r(s) = \frac{\tilde{F}(s+r)}{\frac{s}{s+r} + \frac{r}{s+r}\tilde{F}(s+r)}$ [66] and from here follows the FPTD under Poissonian resetting via the Bromwich integral [68]: $F_r(t) = \frac{1}{2\pi i}\int_{\gamma-i\infty}^{\gamma+i\infty} ds \frac{(s+r)\tilde{F}(s+r)}{s+r\tilde{F}(s+r)} e^{st}$. While an exact evaluation of the integral is difficult, we can obtain the long-time behavior of $F_r(t)$ by looking at the pole of $\tilde{F}_r(s)$ closest to the origin. If $s_{0,r}$ is the pole nearest to zero, then it solves the equation: $0 = s + r\mathcal{L}[e^{-rt}F(t)]$, where $\mathcal{L}$ denotes the Laplace transform, leading to $F_r(t) \approx e^{s_{0,r}t}$. In other words, the long-time behavior of the FPTD under Poissonian restarts exhibits exponential decay. We compare the analytical estimate of the FPTD with its numerical counterpart for a

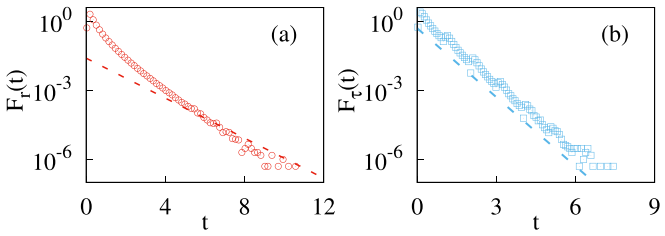

FIG. 5. Comparing the FPTDs: (a) $F_r(t)$ under Poissonian restarts, and (b) $F_\tau(t)$ under sharp resetting. The symbols are numerically estimated and the dashed lines represent the analytical approximations obtained via inverting the Laplace representations. The periodic behavior of $F_\tau(t)$ is evident. Parameter values are $c_1 = 1$, $c_2 = 2$, $D = 1$.

representative value of $r = 1$ in Fig. 5(a). We find a reasonable agreement between the two as $s_{0,r} \approx -1.0$ (analytically) while its numerical value is $s_{0,r} \approx -1.25$ [see Fig. 5(a) for comparison], a difference of about 20%. With an exact representation of the Laplace transform $\tilde{F}_r(s)$ unavailable, we cannot provide a plausible explanation for this difference here.

On the other hand, for sharp resetting, the FPTD in Laplace domain reads [56,65]:

$$\tilde{F}_\tau(s) = \frac{\int_0^\tau dt\, F(t) e^{-st}}{1 - e^{-s\tau} \int_\tau^\infty dt\, F(t)}, \tag{9}$$

and its Laplace inversion at long times is determined by the pole $s_{0,\tau}$ of $\tilde{F}_\tau(s)$ closest to zero. Furthermore, if we consider a periodic function with a period τ, that is, $h(t+\tau) = h(t)$, then its Laplace transform reads [69,70]: $\tilde{h}(s) = \frac{\int_0^\tau dt\, h(t) e^{-st}}{1 - e^{-s\tau}}$. Comparing this with Eq. (9) shows that it is similar to $\tilde{F}_\tau(s)$, except for the appearance of the term $\int_\tau^\infty dt\, F(t)$ in the denominator of the fraction defining $\tilde{F}_\tau(s)$ in Eq. (9). This implies that the FPTD $F_\tau(t)$ exhibits a periodic structure with an exponentially decaying envelope. Furthermore, this behavior of the FPTD is generic to any first passage process under sharp resetting, and not limited to the Bernoulli trial under consideration. Here, however, we can make a comparison of our analytical approximation against numerical calculations. We see from Fig. 5(b) that $F_\tau(t)$ does exhibit a periodic behavior with an envelope tracing the curve $F_\tau(t) \approx e^{-2.3t}$ (obtained via Laplace inversion) with the same period τ (= 1), as explained above.

Conclusions. If we ask ourselves one question, what is the quintessential problem in life, we will almost always come to one answer: the problem is choice. Motivated by this line of thought, we study a Bernoulli trial under restarts. Considering the well-studied capture problem in which a hungry lion pursues a lamb in presence of a safe haven for the lamb we study the properties of success probability and mean escape time for the lamb to make it to the safe haven under Poissonian and sharp resetting. We find that the success probability decreases monotonically as a function of the restart rate ρ, though the nature of decay is different for the two resetting protocols. The mean time of successful completion, however, exhibits a non-monotonic dependence on $1/\rho$, and furthermore, a bimodal behavior for sharp resetting. The optimal value of mean restart time at which the mean success time is minimal, exhibits a dynamical phase transition, with the resetting transition being continuous for Poissonian restarts and discontinuous for sharp restarts. The ubiquity of Bernoulli trials and knowing the way stochastic resetting affects its properties is important in developing insights about chemical selectivity, protein folding, etc. Furthermore, the distinct nature of the resetting transitions for the two protocols, viz. Poisson and sharp possess a natural question: is this generic or specific to systemic details? In other words, what happens to the nature of restart transition if we change the restart protocol, say, power law distributed reset times? To answer this question, let us consider $P^\gamma(R) = \frac{\gamma r}{(1+rR)^{1+\gamma}}$ with $r, \gamma > 0$. This leads to

$$p_\gamma = \frac{\int_0^\infty dt\, \frac{F_1(t)}{(1+rt)^\gamma}}{\int_0^\infty dt\, \frac{F(t)}{(1+rt)^\gamma}}, \tag{10a}$$

$$\langle T_\gamma^s \rangle = \frac{\int_0^\infty dt\, F(t) \frac{(1+rt)^\gamma - 1 - \gamma rt}{r(\gamma-1)(1+rt)^\gamma}}{\int_0^\infty dt\, \frac{F(t)}{(1+rt)^\gamma}} + \frac{\int_0^\infty dt\, \frac{tF_1(t)}{(1+rt)^\gamma}}{\int_0^\infty dt\, \frac{F_1(t)}{(1+rt)^\gamma}}. \tag{10b}$$

This implies that the success probability p_γ exists $\forall\, \gamma > 0$, that is, even when $P^\gamma(R)$ does not possess any finite moments. On the other hand, the conditional MFPT for a successful completion $\langle T_\gamma^s \rangle$, exists only for $\gamma > 1$ and possesses a unique global minima analogous to Poissonian restarts (see Ref. [64] for details). Does this mean that discontinuous transitions are unique to sharp resetting? Or are there some generic conditions imposed on the restart time distribution $P(R)$ leading to a discontinuous transition. Furthermore, we have limited our analysis to a system of two vicious walkers on a line. It would be interesting to see how the results of the present work modify when generalizing to $N > 2$ (vicious) Brownian particles on a line [71,72]. We pursue these and related questions in future works.

Acknowledgments. R.K.S. thanks the Israel Academy of Sciences and Humanities (IASH) and the Council of Higher Education (CHE) Fellowship. T.S. acknowledges financial support by the German Science Foundation (DFG, Grant No. ME 1535/12-1). T.S. is supported by the Alliance of International Science Organizations (Project No. ANSO-CR-PP-2022-05). T.S. is also supported by the Alexander von Humboldt Foundation. S.S. thanks Kreitman Fellowship and HPC facility at Ben-Gurion University. We thank the anonymous reviewer for insightful suggestions.

[1] A. W. F. Edwards, Int. Stat. Rev. **51**, 73 (1983).
[2] S. Condamin, O. Bénichou, and M. Moreau, Phys. Rev. E **75**, 021111 (2007).
[3] S. Condamin, V. Tejedor, R. Voituriez, O. Bénichou, and J. Klafter, Proc. Natl. Acad. Sci. USA **105**, 5675 (2008).
[4] O. Benichou, T. Guérin, and R. Voituriez, J. Phys. A: Math. Theor. **48**, 163001 (2015).
[5] I. Lohmar and J. Krug, J. Stat. Phys. **134**, 307 (2009).
[6] E. Abad, S. B. Yuste, and K. Lindenberg, Phys. Rev. E **86**, 061120 (2012).

[7] S. B. Yuste, E. Abad, and K. Lindenberg, Phys. Rev. Lett. **110**, 220603 (2013).
[8] D. Campos, E. Abad, V. Méndez, S. B. Yuste, and K. Lindenberg, Phys. Rev. E **91**, 052115 (2015).
[9] B. Meerson and S. Redner, Phys. Rev. Lett. **114**, 198101 (2015).
[10] J. Rehbein and B. K. Carpenter, Phys. Chem. Chem. Phys. **13**, 20906 (2011).
[11] S. V. Solomatin, M. Greenfeld, S. Chu, and D. Herschlag, Nature (London) **463**, 681 (2010).
[12] C. A. Pierse and O. K. Dudko, Phys. Rev. Lett. **118**, 088101 (2017).
[13] P. L. Krapivsky, S. Redner, and E. Ben-Naim, *A Kinetic View of Statistical Physics* (Cambridge University Press, Cambridge, 2010).
[14] D. Bernardi and B. Lindner, Phys. Rev. Lett. **128**, 040601 (2022).
[15] G. Oshanin, O. Vasilyev, P. L. Krapivsky, and J. Klafter, Proc. Natl. Acad. Sci. USA **106**, 13696 (2009).
[16] S. Redner and P. L. Krapivsky, Amer. J. Phys. **67**, 1277 (1999).
[17] S. Redner and O. Bénichou, J. Stat. Mech. (2014) P11019.
[18] D. Ben-Avraham, B. M. Johnson, C. A. Monaco, P. L. Krapivsky, and S. Redner, J. Phys. A: Math. Gen. **36**, 1789 (2003).
[19] S. Redner, *A Guide to First-Passage Processes* (Cambridge University Press, Cambridge, 2001).
[20] A. Gabel, S. N. Majumdar, N. K. Panduranga, and S. Redner, J. Stat. Mech. (2012) P05011.
[21] V. Elgart and A. Kamenev, Phys. Rev. E **70**, 041106 (2004).
[22] M. Assaf and B. Meerson, Phys. Rev. E **74**, 041115 (2006).
[23] M. Assaf and B. Meerson, Phys. Rev. E **75**, 031122 (2007).
[24] M. Khasin and M. I. Dykman, Phys. Rev. Lett. **103**, 068101 (2009).
[25] I. Nayak, D. Das, and A. Nandi, Phys. Rev. Res. **2**, 013114 (2020).
[26] S. Belan, Phys. Rev. Lett. **120**, 080601 (2018).
[27] M. E. Fisher, J. Stat. Phys. **34**, 667 (1984).
[28] D. A. Huse and M. E. Fisher, Phys. Rev. B **29**, 239 (1984).
[29] I. Ispolatov, P. L. Krapivsky, and S. Redner, Phys. Rev. E **54**, 1274 (1996).
[30] A. J. Bray, S. N. Majumdar, and G. Schehr, Adv. Phys. **62**, 225 (2013).
[31] P. J. Forrester, J. Stat. Phys. **56**, 767 (1989).
[32] M. Katori and H. Tanemura, Phys. Rev. E **66**, 011105 (2002).
[33] J. Baik, Commun. Pure Appl. Math. **53**, 1385 (2000).
[34] J. W. Essam and A. J. Guttmann, Phys. Rev. E **52**, 5849 (1995).
[35] J. N. Pedersen, M. S. Hansen, T. Novotnỳ, T. Ambjörnsson, and R. Metzler, J. Chem. Phys. **130**, 164117 (2009).
[36] J. Cardy and U. C. Täuber, Phys. Rev. Lett. **77**, 4780 (1996).
[37] M. E. Fisher and M. P. Gelfand, J. Stat. Phys. **53**, 175 (1988).
[38] G. Schehr, S. N. Majumdar, A. Comtet, and J. Randon-Furling, Phys. Rev. Lett. **101**, 150601 (2008).
[39] A. Kundu, S. N. Majumdar, and G. Schehr, J. Stat. Phys. **157**, 124 (2014).
[40] J. Cardy and M. Katori, J. Phys. A: Math. Gen. **36**, 609 (2003).
[41] P. L. Krapivsky and S. Redner, J. Phys. A: Math. Gen. **29**, 5347 (1996).
[42] I. Nayak, A. Nandi, and D. Das, Phys. Rev. E **102**, 062109 (2020).
[43] M. R. Evans and S. N. Majumdar, Phys. Rev. Lett. **106**, 160601 (2011).
[44] M. R. Evans and S. N. Majumdar, J. Phys. A: Math. Theor. **51**, 475003 (2018).
[45] S. Gupta, S. N. Majumdar, and G. Schehr, Phys. Rev. Lett. **112**, 220601 (2014).
[46] S. N. Majumdar, S. Sabhapandit, and G. Schehr, Phys. Rev. E **91**, 052131 (2015).
[47] R. K. Singh, K. Gorska, and T. Sandev, Phys. Rev. E **105**, 064133 (2022).
[48] S. Ahmad, I. Nayak, A. Bansal, A. Nandi, and D. Das, Phys. Rev. E **99**, 022130 (2019).
[49] S. Ahmad, K. Rijal, and D. Das, Phys. Rev. E **105**, 044134 (2022).
[50] J. Masoliver, Phys. Rev. E **99**, 012121 (2019).
[51] V. Domazetoski, A. Masó-Puigdellosas, T. Sandev, V. Méndez, A. Iomin, and L. Kocarev, Phys. Rev. Res. **2**, 033027 (2020).
[52] R. K. Singh, T. Sandev, A. Iomin, and R. Metzler, J. Phys. A: Math. Theor. **54**, 404006 (2021).
[53] M. R. Evans and S. N. Majumdar, J. Phys. A: Math. Theor. **47**, 285001 (2014).
[54] A. Pal, S. Kostinski, and S. Reuveni, J. Phys. A: Math. Theor. **55**, 021001 (2022).
[55] A. Pal, A. Kundu, and M. R. Evans, J. Phys. A: Math. Theor. **49**, 225001 (2016).
[56] A. Pal and S. Reuveni, Phys. Rev. Lett. **118**, 030603 (2017).
[57] A. Chechkin and I. M. Sokolov, Phys. Rev. Lett. **121**, 050601 (2018).
[58] I. Eliazar and S. Reuveni, J. Phys. A: Math. Theor. **53**, 405004 (2020).
[59] I. Eliazar and S. Reuveni, J. Phys. A: Math. Theor. **54**, 355001 (2021).
[60] I. Eliazar and S. Reuveni, J. Phys. A: Math. Theor. **54**, 125001 (2021).
[61] I. I. Eliazar and S. Reuveni, J. Phys. A: Math. Theor. **56**, 024002 (2023).
[62] I. I. Eliazar and S. Reuveni, J. Phys. A: Math. Theor. **56**, 024003 (2023).
[63] A. Pal and V. V. Prasad, Phys. Rev. E **99**, 032123 (2019).
[64] See Supplemental Material at http://link.aps.org/supplemental/10.1103/PhysRevE.108.L052106 for numerical solution and power law restarts.
[65] R. K. Singh and S. Singh, Phys. Rev. E **106**, 064118 (2022).
[66] S. Reuveni, Phys. Rev. Lett. **116**, 170601 (2016).
[67] W. H. Press, S. A. Teukolsky, W. T. Vetterling, and B. P. Flannery, *Numerical Recipes in Fortran 77* (Cambridge University Press, Cambridge, 1986).
[68] G. B. Arfken and H. J. Weber, *Mathematical Methods for Physicists* (Harcourt, San Diego, 1995).
[69] M. R. Spiegel, *Theory and Problems of Laplace Transforms* (McGraw-Hill, New York, 1965).
[70] J. L. Schiff, *The Laplace Transform: Theory and Applications* (Springer Science & Business Media, Berlin, 1999).
[71] M. Biroli, S. N. Majumdar, and G. Schehr, Phys. Rev. E **107**, 064141 (2023).
[72] O. Vilk, M. Assaf, and B. Meerson, Phys. Rev. E **106**, 024117 (2022).